K. Omasa • H. Saji
S. Youssefian • N. Kondo (Eds.)

Air Pollution and Plant Biotechnology

Prospects for Phytomonitoring and Phytoremediation

Springer

15
Image Instrumentation of Chlorophyll *a* Fluorescence for Diagnosing Photosynthetic Injury

Kenji Omasa and Kotaro Takayama

Department of Biological and Environmental Engineering, Graduate School of Agricultural and Life Sciences, The University of Tokyo, Yayoi 1-1-1, Bunkyo-ku, Tokyo 113-8657, Japan

1. Introduction

Environmental stress factors such as air pollutants, agricultural chemicals, water deficit, chilling, and UV light can affect the health of plants (Larcher 1995; Kramer and Boyer 1995; Yunus and Iqbal 1996; De Kok and Stulen 1998). The first symptoms to appear are decreases in photosynthesis and growth. Later symptoms include visible injury of leaves and withering. In recent years forest decline, which may be due to environmental stress factors including meteorological changes, has been widely reported (Schulze et al. 1989; Larcher 1995; Sandermann et al. 1997).

Recent advances in imaging of physiological functions of intact plants to diagnose early abnormal symptoms are remarkable (Omasa and Aiga 1987; Omasa 1990, 2000; Hashimoto et al. 1990; Häder 1992, 2000; Lichtenthaler 1996). For example, thermal imaging (Omasa and Aiga 1987; Omasa and Croxdale 1992; Omasa 1994, this volume; Jones 1999), which gives information on stomatal response and gas exchange, including transpiration, photosynthesis, and absorption of air pollutants, has been applied to remote sensing of outdoor trees and to spatial analysis of physiological functions of leaves in indoor experiments. Multispectral image analyses of leaf reflection (Omasa and Aiga 1987; Omasa 1990, 2000;

Air Pollution and Plant Biotechnology
–Prospects for Phytomonitoring and Phytoremediation–
Edited by K. Omasa, H. Saji, S. Youssefian, and N. Kondo

Wessman 1990; Chappelle et al. 1992; Renxz 1999), and steady-state fluorescence (Lichtenthaler 1996; Kim et al. 1996, 1997, this volume; Saito et al. 1997) have been used for early detection of alteration and bleaching of plant pigments related to photosynthetic injuries. Laser-induced fluorescence (LIF) may be effective for obtaining specific information on changes in cell walls bound by phenolics, compounds in vacuoles, and other fluorophores in living mesophylls in addition to the foregoing information.

Meanwhile, originally developed by Omasa et al. (1987) and Daley et al. (1989), the techniques of image analysis of chlorophyll (Chl) *a* fluorescence of plant leaves in situ has been widely used as a sensitive and nondestructive way to assess the functional state of the photosynthetic apparatus. These techniques are used for early detection of changes in patchy stomatal response and photosynthetic activity caused by abiotic stress factors such as air pollutants, low concentrations of O_2, water deficit, UV light, chilling, and agricultural chemicals (Omasa et al. 1987, 1991, 2001; Daley et al. 1989; Omasa and Shimazaki 1990; Siebke and Weis 1995a; Rolfe and Scholes 1995; Takayama et al. 2000) and biotic stress factors (Balachandran et al. 1994; Osmond et al. 1998). These techniques can also be used to analyze the development of the photosynthetic apparatus of attached leaves and cultured tissues (Croxdale and Omasa 1990a, 1990b; Omasa 1992). Recently, field-portable imaging systems (Daley 1995; Osmond et al. 1998; this volume) and the LIF imaging system (Omasa 1988, 1998) for remote measurement of Chl fluorescence induction have been developed.

In the following section, examples of the diagnosis of photosynthetic dysfunction of plants caused by environmental stress factors such as air pollutants and agricultural chemicals using techniques of image analysis of Chl *a* fluorescence are reviewed.

2. Chlorophyll *a* Fluorescence

2.1 Chlorophyll Fluorescence Induction

Figure 1 shows an excitation and emission matrix of steady-state fluorescence of a healthy cucumber (*Cucumis sativus* L. cv. Sharp7) leaf. When the leaf is irradiated with visible rays of light (about 380 to 600 nm), fluorescence with very strong intensity in the spectral range of about 660 to 770 nm is emitted from Chl *a*. Because Chl *a* fluorescence is the reemission of light energy trapped by antenna chlorophyll and is not used in the photochemical reaction, fluorescence intensity depend on the magnitude of the photochemical reaction (Papageorgiou 1975; Lichtenthaler 1988; Krause and Weis 1991; Govindjee 1995). Rapid changes in the intensity of Chl *a* fluorescence (peak wavelength, 683 nm) emitted from photosystem II (PSII) antenna chlorophyll during a dark-light transition (Chl

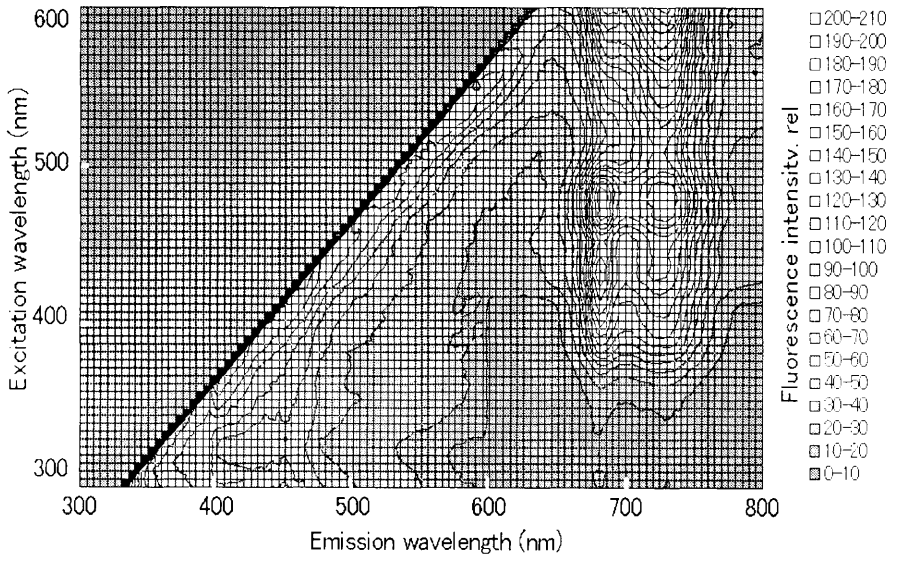

Fig. 1. Matrix of excitation and emission of steady-state fluorescence of a healthy cucumber leaf measured by a fluorescence spectrophotometer (Hitachi F-4500)

fluorescence induction, CFI) reflect the various reactions of photosynthesis, especially those of the photosynthetic electron transport system. This phenomenon is wellknown as the Kautsky effect (Kautsky and Hirsch 1931).

Figure 2 shows CFI transients of a healthy cucumber (*Cucumis sativus* L. cv. Natsusairaku) leaf under different intensities of actinic blue-green light. These measurements clearly revealed the typical CFI transients with inflection points labeled as O, I, D, P, S, M, and T (Papageorgiou and Govindjee 1968; Munday and Govindjee 1969a, 1969b) under light intensities from 50 to 200 μmol photons m^{-2} s^{-1}. The fluorescence increases from O (origin, not shown) to I (inflection or intermediary peak), decreases to D (dip), and increases to P (peak); this is called the fast phase. The fluorescence decreases from P to S (quasi-steady state), and declines to T (terminal steady state) via M (a maximum) (Govindjee 1995); this is called the slow phase.

The fast phase takes a maximum of a few seconds after the start of irradiation with actinic light, although the appearance is faster with increased light intensity. It is closely correlated with the redox reactions of Q_A (Krause and Weis 1991). Because Q_A is the primary electron acceptor of PSII, fluorescence intensity is low when Q_A is oxidized, and high when Q_A is reduced, in the fast phase of CFI. The transient OI represents the photoreduction of Q_A by the PSII reaction center; ID represents rapid oxidation of Q_A by plastoquinone (PQ) pool and photosystem I

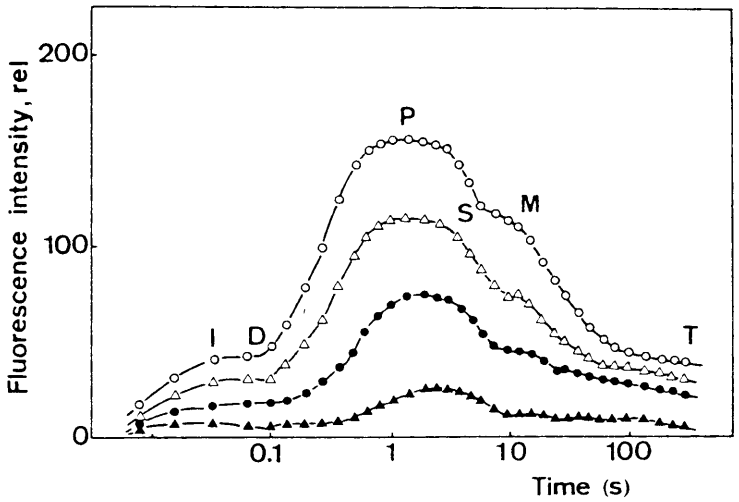

Fig. 2. Chlorophyll fluorescence induction (CFI) transients of a small area (about 1 mm^2) of a healthy cucumber leaf measured under different intensities of actinic blue-green light (Omasa et al. 1987). Intensities of actinic light (○, 200; △, 150; ●,100; ▲,50 μmol photons m^{-2} s^{-1}) were changed by xenon lamps with blue glass filters (380 to 620 nm). Fluorescence was measured by a CCD camera system with an interference filter (683 nm; half-band width, 10 nm) (see Fig.4)

(PSI); and DP indicates the photoreduction of Q_A by the PSII reaction linked to the water-splitting enzyme system. The transient from P to T in the slow phase requires a couple of minutes. The change includes two components, photochemical quenching and nonphotochemical quenching. It may also reflect an interaction between electron transport and carbon fixation.

The CFI transient represents a complex polyphasic process in which the details depend on experimental conditions. We should note that the CFI transient is influenced by (1) PSII cooperativity, (2) PSII heterogeneity, (3) size of the PQ pool and rate of its reoxidation, (4) rate of electron transport beyond PSI including carbon metabolism, and (5) rate of electron donation to P^+_{680} (Krause and Weis 1991).

2.2 Chlorophyll Fluorescence Quenching

Under continuous light, fluorescence intensity shows a lower value than its maximum. "Chl fluorescence quenching" denotes all processes that lower the fluorescence intensity. The quenching consists of photochemical and

nonphotochemical components. Photochemical quenching is closely correlated with the oxidation state of Q_A. Nonphotochemical quenching is an index of the ability of the photosynthetic apparatus to generate a high *trans*-thylakoid pH gradient, to sustain electron transport, and to waste excess excitation energy as heat. By means of a saturation light pulse, it is possible to quantitatively estimate both photochemical and nonphotochemical quenching (Quick and Horton 1984; Schreiber et al. 1986; Krause and Weis 1991; Siebke and Weis 1995a, 1995b; Govindjee 1995). This fluorescence analysis is called the saturation pulse method.

Figure 3 shows a schematic diagram for measuring both CFI images and pulse-saturated fluorescence images. After 1 h dark, the leaf is irradiated with the saturation light pulse, and F_m image is measured. After the leaf is kept in the dark for 30 min, CFI images (fluorescence intensities: F_I at I, F_D at D, F_P at P, F_S at S, F_M at M, and F_T at T) are measured under actinic light. After confirmation of steady-state fluorescence under actinic light, F and F_m' images are measured just before and during irradiation of the saturation light pulse, respectively.

As quenching parameters, q_P, q_N, NPQ (nonphotochemical quenching), and Φ_{PSII} (quantum yield of PSII electron transport) have been widely used (Schreiber et al. 1986; Bilger and Björkman 1990; Kooten and Snel 1990; Krause and Weis

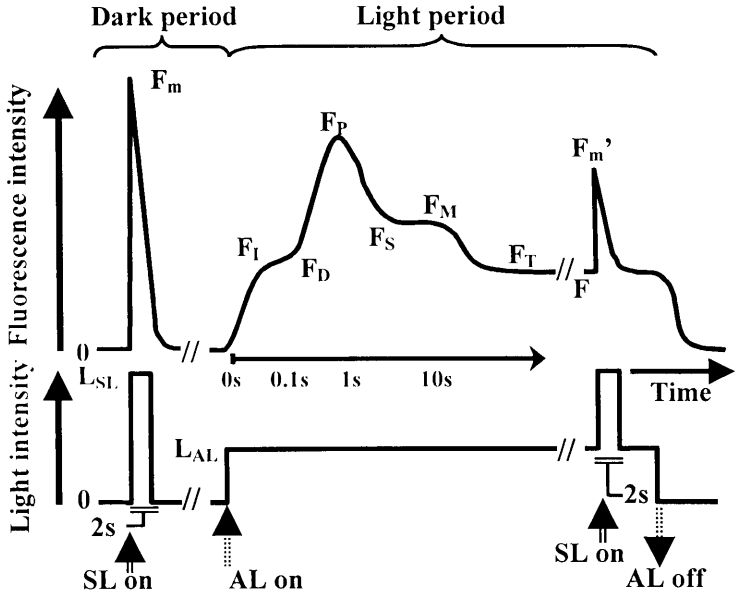

Fig. 3. Schematic diagram for measuring both CFI images and pulse-saturated fluorescence images

1991; Genty and Meyer 1995; Rolfe and Scholes 1995; Siebke and Weis 1995a; Osmond et al. 1998). These parameters are calculated from fluorescence yield images obtained from fluorescence intensity images. Fluorescence yield is the quantum yield of Chl *a* fluorescence. The absolute fluorescence yield is obtained from the total number of photons emitted divided by the total number of photons absorbed (Govindjee 1995). When actinic light and saturation light pulse are absorbed in an essentially identical manner by Chl, relative fluorescence yield images (Φ_{Fm}, Φ_F, and $\Phi_{Fm'}$) are calculated by

$$\Phi_{Fm} \cong F_m/L_{SL} \tag{1}$$

$$\Phi_F \cong F/L_{AL} \tag{2}$$

$$\Phi_{Fm'} \cong F_m'/L_{SL} \tag{3}$$

where F_m is the maximal fluorescence intensity (dark), F is the steady-state fluorescence intensity under actinic light, F_m' is the maximal fluorescence intensity under actinic light, L_{SL} is the intensity of saturation light pulse, and L_{AL} is the intensity of actinic light (Schreiber 1986; Rolfe and Scholes 1995).

Photochemical quenching is caused by the oxidized state of the primary acceptor (Q_A) of PSII. The coefficient for photochemical quenching, q_P, represents the proportion of excitons captured by open traps and being converted to chemical energy in the PSII reaction center (Krause and Weis 1991). q_P is calculated by

$$q_P = (\Phi_{Fm'}-\Phi_F)/(\Phi_{Fm'}-\Phi_{F0'}) \cong (\Phi_{Fm'}-\Phi_F)/(\Phi_{Fm'}-0.2\times\Phi_{Fm}) \tag{4}$$

where Φ_{Fm} is the maximal fluorescence yield (dark), that is, fluorescence yield with all PSII reaction centers closed (q_P=0) and all nonphotochemical quenching processes are at a minimum (q_N=0), $\Phi_{Fm'}$ is the maximal fluorescence yield (light), that is, fluorescence yield with all PSII reaction centers closed in any light-adapted state (q_P=0 and $q_N \geqq 0$), and $\Phi_{F0'}$ is the minimal fluorescence yield (light), that is, fluorescence yield with all PSII reaction centers open in any light adapted state (q_P=1 and $q_N \geqq 0$). $\Phi_{F0'}$ excited by the measuring beam of the PAM fluorometer is too weak to measure with the ordinary video system. Therefore, $\Phi_{F0'}$ is nearly constant and approximately 0.2 × Φ_{Fm} (Schreiber et al. 1986; Daley et al. 1989; Osmond et al. 1998).

Nonphotochemical quenching is caused in vivo by several mechanisms. However, most of nonphotochemical quenching has been found to be correlated to the energization of the thylakoids because of the build-up of a transmembrane pH gradient. The coefficient for nonphotochemical quenching, q_N, represents the proportion of the nonphotochemical quenching in all fluorescence quenching. q_N is computed by

$$q_N = 1-(\Phi_{Fm'}-\Phi_{F0'})/(\Phi_{Fm}-\Phi_{F0}) \cong (\Phi_{Fm}-\Phi_{Fm'})/(0.8\times\Phi_{Fm}) \tag{5}$$

where Φ_{F0} is the minimal fluorescence yield (dark), that is, fluorescence yield with all PSII reaction centers open while the photosynthetic membrane is in the nonenergized state (dark- or low-light-adapted q_P=1 and q_N=0), nearly constant, and approximately 0.2 × Φ_{Fm} as Φ_{F0} is equal to $\Phi_{F0'}$ (Schreiber et al. 1986; Daley et al. 1989; Osmond et al. 1998).

Knowledge of $\Phi_{F0'}$ is indispensable in order to calculate q_P and q_N. However, the determination of $\Phi_{F0'}$ may be problematic, particularly under field conditions. Hence, NPQ as a nonphotochemical quenching parameter which does not require the determination of $\Phi_{F0'}$ was developed. NPQ is computed by

$$NPQ = (\Phi_{Fm}-\Phi_{Fm'})/\Phi_{Fm'} \tag{6}$$

Furthermore, quantum yield of PSII electron transport, Φ_{PSII}, as a parameter for the assessment of the proportion of light energy absorbed by PSII and used in photosynthetic electron transport was developed. Φ_{PSII} can be also calculated by the following expression without determining $\Phi_{F0'}$.

$$\Phi_{PSII} = (\Phi_{Fm'}-\Phi_F)/\Phi_{Fm'} = \Delta\Phi_F/\Phi_{Fm'} \tag{7}$$

The product of Φ_{PSII} and irradiance is linearly related to CO_2 assimilation rate under suitable measuring conditions. Φ_{PSII} is used as an indicator of the rate of photosynthesis (Genty et al. 1989).

3. Image Instrumentation System

Figure 4 shows a diagram of the laser-induced fluorescence (LIF) image instrumentation system for analyzing Chl fluorescence and photographs of scanning argon laser. This system can be used to measure CFI images by stimulating the photosynthetic apparatus with actinic light from a scanning argon laser (457.9, 514.5 nm) in addition to halogen or xenon lamps with blue glass filters (380 to 620 nm). In the scanning laser system, a beam from an argon laser (800 mW) is scanned horizontally by a polygon laser scanner (4 in Fig. 4) and vertically by a galvanometer scanner (6). The scan rate is controlled by synchronization with the signal from a camera controller or a computer system. The maximum scanning rate is 30 s^{-1}. Another galvanometer scanner (3) and a

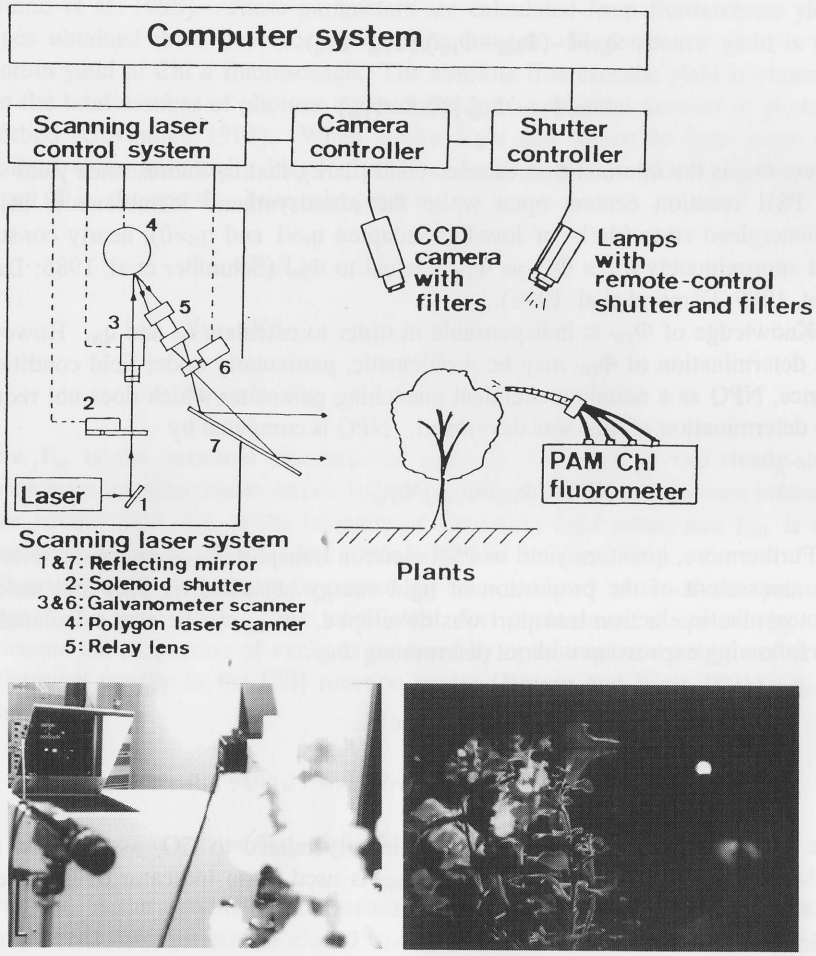

Fig. 4. Diagram and photographs of laser-induced fluorescence (LIF) image instrumentation system for analyzing CFI transients (Omasa 1988, 1998)

solenoid shutter (2) are used to remove the retrace line in the vertical scan. The left-hand photograph in Fig. 4 shows the scanning laser and the xenon lamp projector, and the right-hand photograph shows a plant irradiated by the scanning laser. The scanning laser enables measurement of plants from a greater distance than with the xenon lamp.

Figure 5 shows a comparison between CFI transients of a small area (about 1

mm^2) of a healthy sunflower (*Helianthus annuus* L. cv. Russian Mammoth) leaf measured in situ with the argon laser (LIF) and CFI transients measured with blue-green actinic light from the xenon lamp projectors at three different intensities of actinic light. Before the CFI measurement, the plant leaf was placed in the dark and allowed to adapt for 20 min. The fluorescence was continuously measured by a highly sensitive CCD (charge-coupled device) camera with uniform sensitivity, afterimage suppression through an interference filter (683 nm; half-band width, 10 nm) and a red-pass filter (>650 nm). A series of images was recorded on a computer or on a digital video recorder and then analyzed by the computer. These CFI transients clearly displayed the typical CFI pattern (see Fig. 2; Papageorgiou 1975; Govindjee 1995). The fluorescence intensity of each transient level and the amplitudes of DP, PS, and MT increased as the light intensity increased, and were almost identical in spite of the difference in light source. Figure 6 shows CFI images induced by the scanning laser taken from a petunia (*Petunia hybrida* L. cv Tytan White) plant. These results confirm that the scanning laser enables clear CFI imaging from a distance.

By the procedure shown in Fig. 3, the system can also be used to analyze Chl fluorescence quenching images as well as CFI images by irradiating with a saturation blue-green light pulse (4000 μmol photons m^{-2} s^{-1}) in addition to the

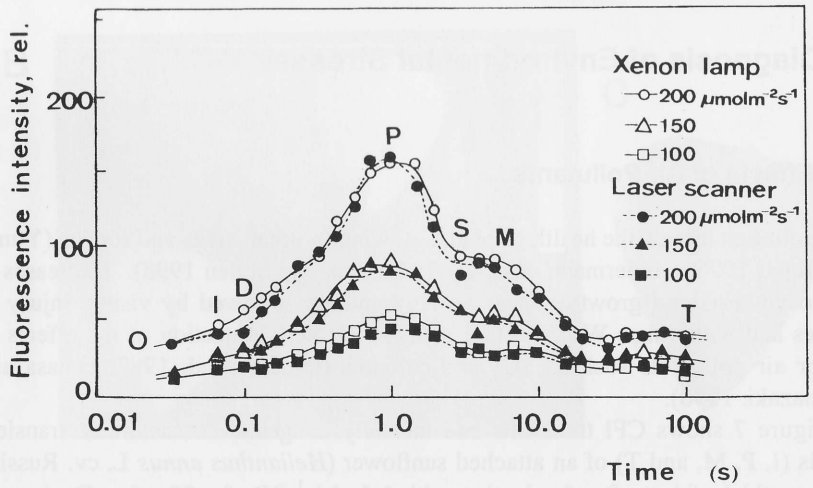

Fig. 5. Comparison between CFI transients of a small area (1 mm^2) of a healthy sunflower leaf measured in situ using the scanning laser (LIF) and CFI transients measured using xenon lamps at different light intensities (Omasa 1988, 1998). The rate of laser scanning was 30 s^{-1}

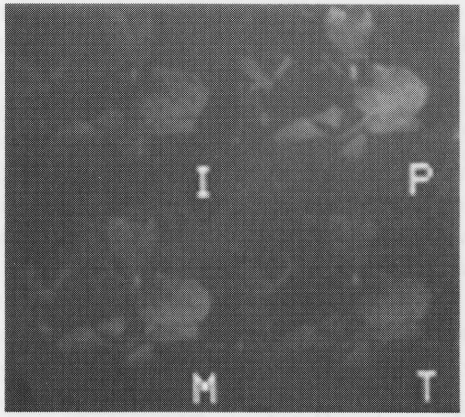

Fig. 6. CFI images at characteristic transient levels (I, P, M, and T) of a petunia plant measured with the scanning laser (Omasa 1988, 1998)

blue-green actinic light (300 μmol photons m^{-2} s^{-1}) from halogen lamps, although it is suitable only for small areas.

4. Diagnosis of Environmental Stresses

4.1 Effects of Air Pollutants

Air pollution affects the health of plants growing in urban areas and forests (Yunus and Iqbal 1996; Sandermann et al. 1997; De Kok and Stulen 1998). Decreases in photosynthesis and growth appear initially and are followed by visible injury of leaves and withering. We used CFI analysis for early detection of the effects of major air pollutants such as SO_2 and oxidants (Omasa et al. 1987; Omasa and Shimazaki. 1990).

Figure 7 shows CFI transients and intensity images at characteristic transient levels (I, P, M, and T) of an attached sunflower (*Helianthus annus* L. cv. Russian Mammoth) leaf just after fumigation with 1.5 μl l^{-1} SO_2 for 30 min. During the fumigation, half of the leaf blade was covered with aluminum foil to shield the leaf from SO_2. This procedure allows comparison between a fumigated area (F) and an unfumigated area (UF) of the same leaf. In the unfumigated area, CFI clearly showed the typical IDPSMT transients (Papageorgiou 1975; Govindjee 1995).

Because the CFI transients observed on dark-light transition of the leaf reflect the partial reactions of photosynthesis, we can detect alterations in the photosynthetic apparatus caused by SO_2 from the changes in CFI transients (Fig. 7A). As shown in Fig. 7B, the image intensity in the fumigated areas differed strikingly from those in the unfumigated areas. Fluorescence intensity in the fumigated area was higher at I, markedly lower at P, and higher at T. The amplitude of fluorescence

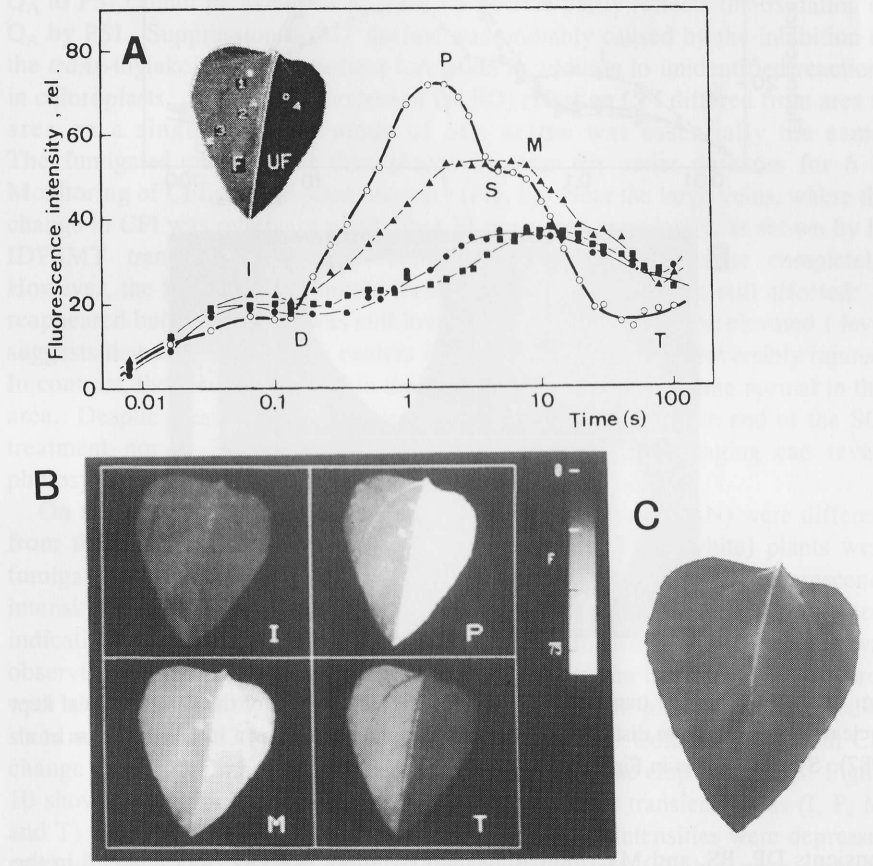

Fig. 7. CFI transients (**A**) and intensity images (**B**) at characteristic transient levels (I, P, M, and T) of an attached sunflower leaf just after 1.5 μl l^{-1} SO_2 fumigation for 30 min (Omasa et al. 1987). Fumigated area (F): ●, interveinal site 1; ▲, site 2, near a large vein; ■, site 3, near a veinlet. Unfumigated area (UF): ○, interveinal site 4. There was no visible injury (**C**)

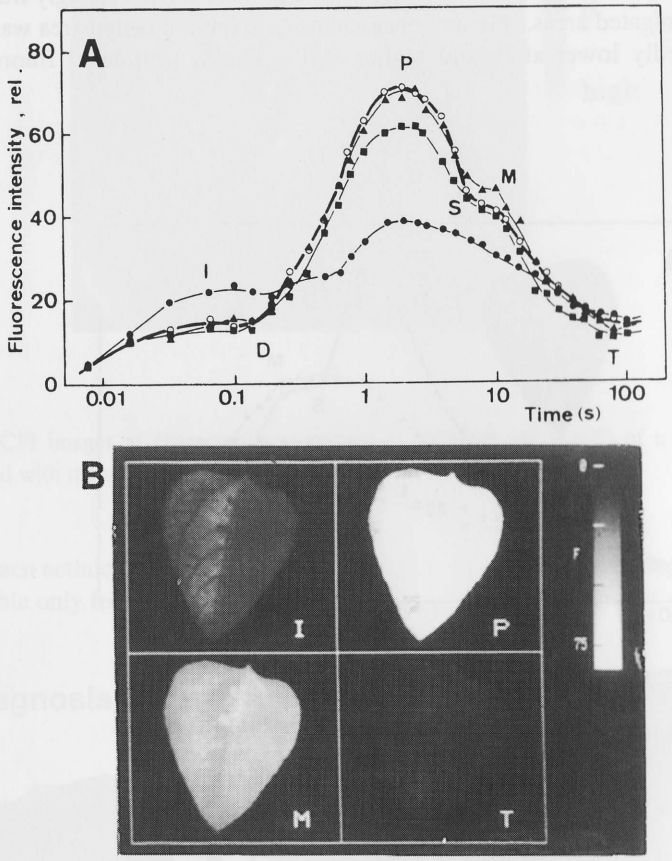

Fig. 8. Recovery of CFI transients (**A**) and intensity images (**B**) of the sunflower leaf kept in clean air for 6 h from disturbances by the SO_2 fumigation shown in Fig.7 (Omasa et al. 1987). Symbols are as in Fig. 7

transients DP, PS, and MT, indicating photosynthetic activity, was reduced in the fumigated areas of the leaf. The changes in intensity and amplitude varied with the location on the leaf surface: the effects of SO_2 were more severe between veins and near veinlets than near large veins. Contrary to the perturbation in the photosynthetic apparatus shown, there was no visible injury in the whole surface of leaf at the end of SO_2 treatment (Fig. 7C) and 2 days later.

The significance of the changes in CFI induced by SO_2 fumigation is as follows

(Omasa et al. 1987). Because fluorescence intensity in the early induction phenomena is regulated by the redox state of Q_A (Papageorgiou 1975; Krause and Weis 1991; Govindjee 1995), the elevated I level suggests that Q_A was brought to the reduced state by SO_2 fumigation. Because the DP rise in CFI reflects photoreduction of Q_A through the reductant from H_2O, a diminished rise of DP was consistent with inactivation of the water-splitting enzyme system. As PS decline involves energy-dependent quenching, its suppression suggested the depression of formation of the *trans*-thylakoid proton gradient was probably caused by the inactivation of the water-splitting enzyme system. However, the possibility that the PS decline was affected by the inhibition of electron flow from Q_A to PSI cannot be excluded because PS decline partly reflects the oxidation of Q_A by PSI. Suppression of MT decline was probably caused by the inhibition of the *trans*-thylakoid proton gradient formation in addition to unidentified reactions in chloroplasts. Although the extent of the SO_2 effect on CFI differed from area to area on a single leaf, the mode of SO_2 action was essentially the same. The fumigated plants were then placed in clean air under darkness for 6 h. Monitoring of CFI showed plant recovery (Fig. 8). Near the large veins, where the change in CFI was relatively small, the CFI recovered completely, as shown by its IDPSMT transient. Near the veinlets, CFI recovered almost completely. However, the fluorescence emitted from the interveinal area was still affected: P reappeared but its intensity was still low, and I was elevated. The elevated I level suggests that the PSII reaction centers in the chloroplasts were irreversibly injured. In contrast, the elevated T level in the quasi-stationary state became normal in this area. Despite these results, however, no injury was visible at the end of the SO_2 treatment nor at 2 days after the treatment. Thus, CFI imaging can reveal photosynthetic damage before symptoms are visible.

On the other hand, CFI responses to peroxyacetyl nitrate (PAN) were different from those to SO_2. Petunia (*Petunia hybrida* L. cv. Tytan white) plants were fumigated with 0.06 μl l^{-1} PAN for 3 h. The CFI transients and fluorescence intensity images observed within 1 h after the fumigation were not affected, indicating that photosynthetic activity was not yet damaged. No visible injury was observed at this time. After the measurement, half of the leaf blade was covered with aluminum foil to prevent light illumination and the plants were allowed to stand under light (130 μmol photons m^{-2} s^{-1}) for 12 h. Consequently, both CFI change and visible injury progressed according to the time elapse (Fig. 9). Figure 10 shows a photograph and CFI images at characteristic transient levels (I, P, M, and T) after the 12 h light treatment. The fluorescence intensities were depressed markedly at visibly injured sites in the irradiated area (a), but were virtually unaffected in the unirradiated area (b). This phenomenon indicates that light played an important role in the phytotoxicity of PAN and that photosynthetic injury depends on bleaching of plant pigments, that is, destruction of cells.

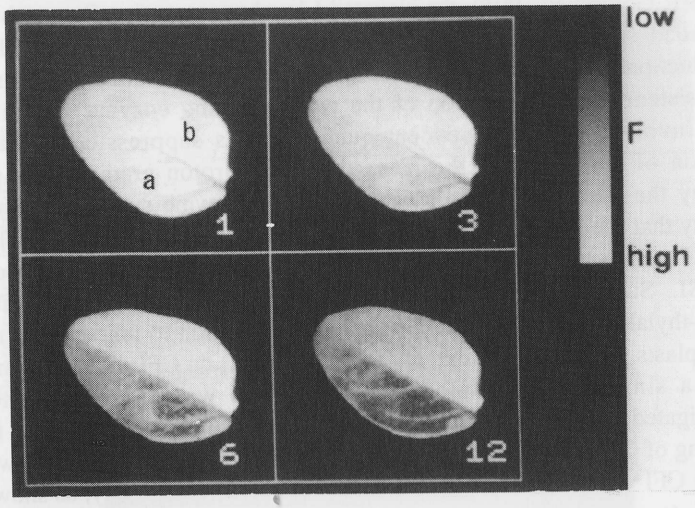

Fig. 9. Changes in intensity image at peak P of CFI of an attached petunia leaf after 0.06 μl l^{-1} peroxyacetyl nitrate (PAN) fumigation for 3 h. Numerals (1, 3, 6, 12) show the elapse of time (h) after the end of fumigation. A, area irradiated under 130 μmol photons m^{-2} s^{-1} after the fumigation; B, unirradiated area

4.2 Effects of Herbicides

Many herbicides inhibit photosynthetic functions of plants. Heterogeneous distribution of photosynthetic inhibition in leaves caused by herbicides has been widely investigated by Chl fluorescence analysis (Daley et al. 1989; Genty and Meyer 1995; Rolfe and Scholes 1995; Takayama et al. 2000; Omasa et al. 2001).

Figure 11 shows CFI and quenching images obtained by a sequence, shown in Fig.3, of kidney bean (*Phaseolus vulgaris* L. cv. Shinedogawa) leaves after treatment with 1/1000 diluted solution of a herbicide, Nekosogi-ace (Rainbow Chemicals), including 6.0% 3-(3,4-dichlorophenyl)-1,1-dimethylurea (DCMU), 3.0% 2,6-dichlorothiobenzamide (DCBN), and 1.0% 3-(5-*tert*-butylisoxazol-3-yl)-1,1-dimethylurea (isouron) from the leafstalk for 20 min. Although the fluorescence intensity was relatively uniform all over the leaf surface before treatment, it was remarkably increased at mesophyll cells around the major veins in several images of CFI and pulse-saturated fluorescence after the treatment. Because DCMU blocks electron transfer from Q_A to PQ, probably by binding to the Q_B site of the D1 protein, the fluorescence rise from O to P in CFI transients is

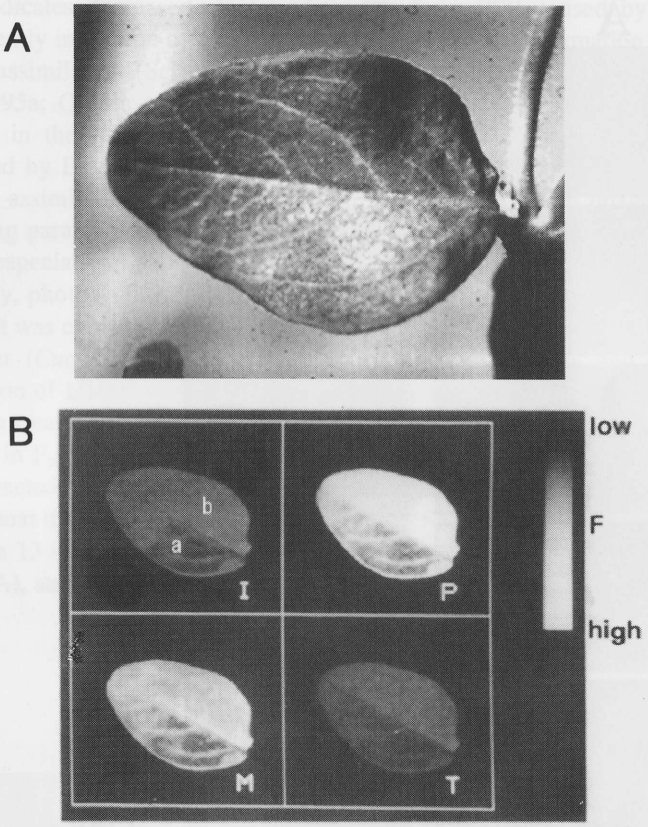

Fig. 10. A photograph (**A**) and CFI images (**B**) at characteristic transient levels (I, P, M, and T) of the attached petunia leaf at 12 h after the end of PAN fumigation shown in Fig.9 (Omasa and Shimazaki 1990). Symbols are as in Fig. 9. Visible injury was observed in irradiated area only (**A**)

much faster in the presence of DCMU than in the absence of the inhibitor (Krause and Weis 1991). Therefore, we could diagnose the fluorescence rise at sites around major veins observed in Fig. 11A as photosynthetic inhibition caused by DCMU in Nekosogi-ace transported with the transpiration stream from the leafstalk. Isouron also might cause fluorescence rise because it blocks the electron transfer. There was no visible injury on the leaf during the measurement (C).

Quenching parameters such as q_P, q_N, NPQ, and Φ_{PSII} calculated by Eqs. 4 to 7 are known as indicators of photochemical and nonphotochemical quenching. Values of nonphotochemical quenching parameters, q_N and NPQ, decreased at

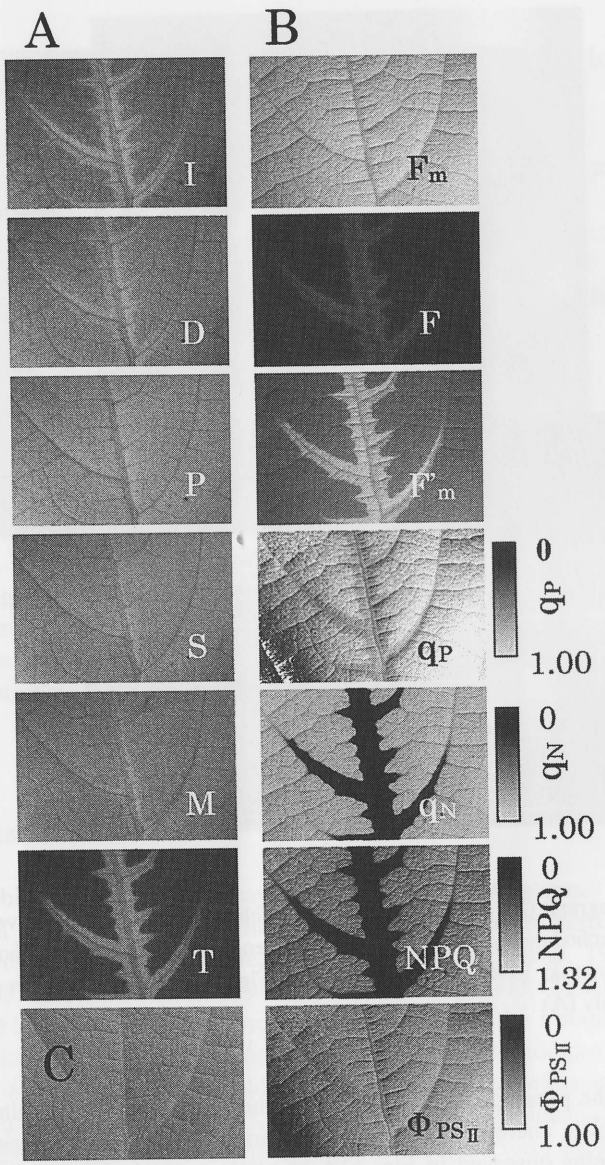

Fig. 11. CFI images (**A**) at characteristic transient levels (I, D, P, S, M, and T) and quenching images (**B**) obtained by a sequence shown in Fig. 3 of a kidney bean leaf after treatment with 1/1000 diluted solution of a herbicide, Nekosogi-ace (Rainbow Chemicals), including 6.0% DCMU, 3.0% DCBN, and 1.0% isouron, from the leafstalk for 20 min (Omasa et al. 2001). There was no visible injury just after the treatment (**C**)

about the same sites around the major veins as inhibition sites in CFI images. This result indicates decreased electron transport from PSII caused by DCMU and consequently inhibition of *trans*-thylakoid proton gradient formation and decrease in CO_2 assimilation (Schreiber et al. 1986; Krause and Weis 1991; Siebke and Weis 1995a; Omasa et al. 2001). However, DCMU inhibition was not clearly detected in the images of q_P and Φ_{PSII}. This result shows that q_P and Φ_{PSII} calculated by Eqs. 4 and 7 are limited as indicators of photochemical inhibition and CO_2 assimilation rate. Consequently, simultaneous use of images of CFI and quenching parameters enables detailed diagnosis of injuries of the photosynthetic system, especially in photochemical inhibition.

Finally, photosynthetic inhibition of intact plants caused by different herbicide treatment was compared. Figure 12 shows F_m, F_m', and NPQ images of an attached cucumber (*Cucumis sativus* L. cv. Sharp7) leaf before (A), and after (B) the application of 1/1000 diluted solution of Nekosogi-ace in soil. After 2 days of the herbicide treatment, mesophyll sites around the major veins showed a remarkable increase in F_m' as compared with noninjured sites. On the other hand, no injuries were detected in the F_m image. The NPQ value showed a decrease in the sites located near the vein.

Figure 13 shows F_m, F_m', and NPQ images of an attached cucumber leaf taken before (A), and after (B) treatment of a foliar application-type herbicide, Roundup

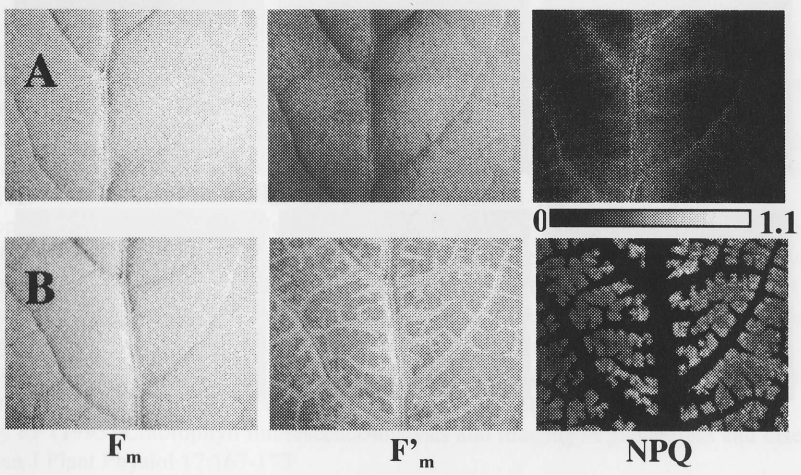

Fig. 12. F_m, F_m', and NPQ images of an attached cucumber leaf before (**A**) and 2 days after (**B**) application of 1/1000 diluted solution of Nekosogi-ace in soil (Takayama et al. 2000). There was no visible injury at 2 days after the treatment

(Monsanto), including 1.0% *N*-(phosphonomethyl)glycine (glyphosate). At 24 h after the treatment, mesophyll sites around the major veins showed a remarkable decrease in F_m and F_m' as compared with noninjured sites, an early symptom of dysfunction in photosynthetic apparatus in these sites. In the NPQ image, the sites around the major veins showed a decrease in NPQ. However, the sites surrounding the low NPQ sites and branches of veins showed a local rise in NPQ.

Photosynthetic inhibition caused by the two types of herbicides was estimated using NPQ images. The manner of appearance of the symptoms differed for the two herbicides, as shown by Figs. 12 and 13. This difference was attributed to the difference in the components of the two herbicides and the methods of application. It was also proven that the inhibition spreads from the sites along the veins for both methods of application. Low values of NPQ in the sites around the major veins predicted low assimilation rates (Daley et al. 1989; Siebke and Weis 1995a; Omasa et al. 2001) and the inhibition of the ability of chloroplasts to generate a *trans*-thylakoid pH gradient, to sustain electron transport, and to dissipate excess excitation energy as heat in these sites (Osmond et al. 1998). However, we cannot explain why the NPQ values increased at the sites surrounding the low-NPQ sites and branches of veins, as shown in Fig. 13.

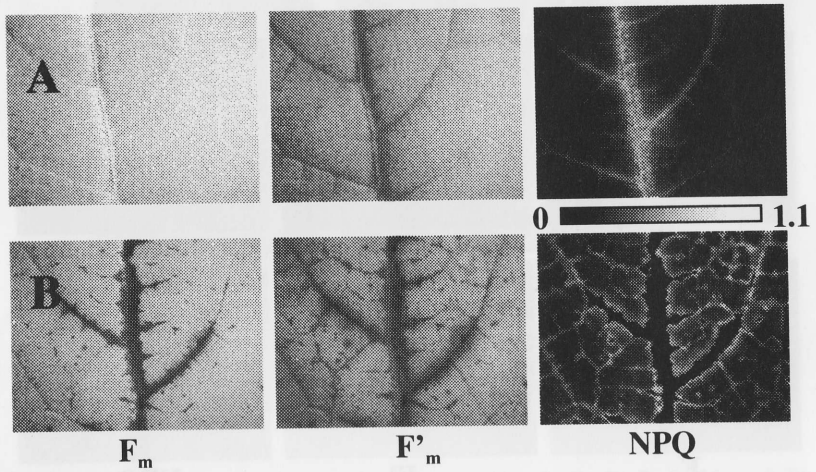

Fig. 13. F_m, F_m', and NPQ images of an attached cucumber leaf before (**A**) and 24 h after (**B**) treatment of a foliar application-type herbicide, Roundup (Monsanto), including 1.0% glyphosate (Takayama et al. 2000). There was no visible injury at 24 h after the treatment

5. Conclusions

We have introduced an image instrumentation system for diagnosing the effects of environmental stress factors such as air pollutants and agricultural chemicals (herbicides) on photosynthetic activity and sites of inhibition in the photosynthetic apparatus of attached leaves. By use of the scanning laser in addition to halogen or xenon lamps, this system enabled diagnosis of photosynthetic functions of plants at a distance from the instrumentation system. In this system, two methods of Chl *a* fluorescence imaging analysis were introduced: CFI analysis and the saturation pulse method. The saturation pulse method can analyze the photosynthetic injuries more quantitatively than by CFI analysis. However, the saturation pulse method requires an evenly distributed high level of photosynthetic active radiation (PAR), which makes it difficult to apply to a large leaf area. In contrast, CFI analysis does not require such a high level of PAR for measurements and is easier to use for examining a large leaf area. Simultaneous use of images of CFI and quenching parameters enables detailed diagnosis of injuries of the photosynthetic system, especially in photochemical inhibition. Although CFI analysis and the saturation pulse method are effective as nondestructive assays of photosynthetic injuries, they are affected by the plant materials and measurement conditions, including pigment contents, leaf age, and surrounding environment. Therefore, it is necessary to use them for accurate assays with other methods such as measurement of CO_2 uptake by assimilation chamber and biochemical analysis.

References

Balachandran S, Osmond CB, Daley PF (1994) Diagnosis of the earliest strain-specific interactions between tobacco mosaic virus and chloroplasts of tobacco leaves *in vivo* by means of chlorophyll fluorescence imaging. Plant Physiol 104:1059-1065

Bilger W, Björkman O (1990) Role of the xanthophyll cycle in photoprotection elucidated by measurements of light-induced absorbance changes, fluorescence and photosynthesis in leaves of Hedera canariensis. Photosynth Res 25:173-185

Chappelle EW, Kim MS, McMurtrey JE III (1992) Ratio analysis of reflectance spectra (RARS): an algorithm for the remote estimation of the concentrations of chlorophyll *a*, chlorophyll *b*, and carotenoids in soybean leaves. Remote Sens Environ 39:239-247

Croxdale JG, Omasa K (1990a) Chlorophyll *a* fluorescence and carbon assimilation in developing leaves of light-grown cucumber. Plant Physiol 93:1078-1082

Croxdale JG, Omasa K (1990b) Patterns of chlorophyll fluorescence kinetics in relation to growth and expansion in cucumber leaves. Plant Physiol 93:1083-1088

Daley PF (1995) Chlorophyll fluorescence analysis and imaging in plant stress and disease. Can J Plant Physiol 17:167-173

Daley PF, Raschke K, Ball JT, et al (1989) Topography of photosynthetic activity of leaves obtained from video images of chlorophyll fluorescence. Plant Physiol 90:1233-1238

De Kok, Stulen I (1998) Responses of plant metabolism to air pollution and global change. Backhuys

Genty B, Meyer S (1995) Quantitative mapping of leaf photosynthesis using chlorophyll fluorescence imaging. Aust J Physiol 22:277–284
Genty B, Briantais JM, Baker NR (1989) The relationship between the quantum yield of photosynthetic electron transport and quenching of chlorophyll fluorescence. Biochim Biophys Acta 990:87-92
Govindjee (1995) Sixty-three years since Kautsky: Chlorophyll *a* fluorescence. Aust J Plant Physiol 22:131-160
Häder DP (eds) (1992) Image analysis in biology. CRC Press
Häder DP (eds) (2000) Image analysis: Methods and applications, 2nd edn. CRC Press
Hashimoto Y, Kramer PJ, Nonami H, et al (1990) Measurement techniques in plant science. Academic Press
Jones HG (1999) Use of thermography for quantitative studies of spatial and temporal variation of stomatal conductance over leaf surface. Plant Cell Environ 22:1043-1055
Kautsky H, Hirsch A (1931) Neue Versuche zur Kohlensäureassimilation. Naturwissenschaftren 19:964
Kim MS, Krizek DT, Daughtry CST, et al (1996) Fluorescence imaging system: application for the assessment of vegetation stresses. SPIE 2959:4-13
Kim MS, Mulchi CL, Daughtry CST, et al (1997) Fluorescence images of soybean leaves grown under increased O_3 and CO_2. SPIE 3059:22-31
Kooten OV, Snel JFH (1990) The use of chlorophyll fluorescence nomenclature in plant stress physiology. Photosynth Res 25:147-150
Kramer PJ, Boyer JS (1995) Water relations of plants and soils. Academic Press
Krause GH, Weis E (1991) Chlorophyll fluorescence and photosynthesis: the basics. Annu Rev Plant Physiol Plant Mol Biol 42:313-349
Larcher W (1995) Physiological plant ecology. Springer
Lichtenthaler HK (1988) Applications of chlorophyll fluorescence. Kluwer
Lichtenthaler HK (1996) Vegetation stress. J Plant Physiol 148:599-644
Munday JCM Jr, Govindjee (1969a) Light-induced changes in the fluorescence yield of chlorophyll *a in vivo*. Ⅲ. The dip and the peak in the fluorescence transient of *Chlorella pyrenoidosa*. Biophysical J 9:1-21
Munday JCM Jr, Govindjee (1969b) Light-induced changes in the fluorescence yield of chlorophyll *a in vivo*. Ⅳ. The effect of pre-illumination on the fluorescence transient of *Chlorella pyrenoidosa*. Biophys J 9:22-35
Omasa K (1988) Image instrumentation of plants using a laser scanner (in Japanese). Proc Annu Meet Jpn Soc Environ Control Biol 1988:14-15
Omasa K (1990) Image instrumentation methods of plant analysis. In: Linskens HF, Jackson JF (eds) Modern methods of plant analysis, vol 11. Springer, New Series, pp 203-243
Omasa K (1992) Image diagnosis of photosynthesis in cultured tissues. Acta Hortic 319:653-658
Omasa K (1994) Diagnosis of trees by portable thermographic system. In: Kuttler W, Jochimsen M (eds) Immissionsökologische Forschung im Wandel der Zeit. Essener Ökologische Schriften, pp 141-152
Omasa K (1998) Image instrumentation of chlorophyll *a* fluorescence. SPIE 3382:91-99
Omasa K (2000) Phytobiological IT in agricultural engineering. Proc XIV Memorial CIGR World Congress 2000:125-132
Omasa K, Aiga I (1987) Environmental measurement: image instrumentation for evaluating pollution effects on plants. In: Singh MG (ed) Systems and control encyclopedia. Pergamon Press, pp 1516-1522
Omasa K, Shimazaki K (1990) Image analysis of chlorophyll fluorescence in leaves. In: Hashimoto Y, Kramer PJ, Nonami H, et al (eds) Measurement technique in plant science. Academic Press, pp 387-401
Omasa K, Croxdale JG (1992) Image analysis of stomatal movements and gas exchange. In: Häder DP (ed) Image analysis in biology. CRC Press, pp 171-193
Omasa K, Shimazaki K, Aiga I, et al (1987) Image analysis of chlorophyll fluorescence transients for diagnosing the photosynthetic system of attached leaves. Plant Physiol 84:748-752
Omasa K, Maruyama S, Matthews MA, et al (1991) Image diagnosis of photosynthesis in water-deficit plants. IFAC Workshop Series 1991, No.1. Pergamon Press, pp 383-388
Omasa K, Takayama K, Goto, E (2001) Image diagnosis of photosynthetic injuries induced by herbicide in plants: comparison of the induction method with the saturation pulse method for chlorophyll a fluorescence analysis (in Japanese with English summary). J Soc High Tech Agric 13:29-37
Osmond CB, Daley PF, Badger MR, et al (1998) Chlorophyll fluorescence quenching during photosynthetic induction in leaves of *Abutilon striatum* dicks. Infected with abutilon mosaic virus, observed with a field-portable imaging system. Bot Acta 111:390-397
Papageorgiou G (1975) Chlorophyll fluorescence: an intrinsic probe of photosynthesis. In: Govindjee (ed) Bioenergetics of photosynthesis. Academic Press, pp 319-371
Papageorgiou G, Govindjee (1968) Light-induced changes in the fluorescence yield of chlorophyll *a in vivo*. Ⅱ. *Chlorella pyrenoidosa*. Biophys J 8:1316-1328
Quick WP, Horton P (1984) Studies on the induction of chlorophyll fluorescence in barley protoplasts. Ⅱ. Resolution of fluorescence quenching by redox state and the *trans*-thylakoid pH gradient. Proc R Soc Lond B 220:371-382
Rencz AN (ed) (1999) Manual of remote sensing, 3rd edn., vol 3. Wiley, New York, p707
Rolfe SA, Scholes JD (1995) Quantitative imaging of chlorophyll fluorescence. New Phytol 131:69-79
Saito Y, Takahashi K, Nomura E, et al (1997) Visualization of laser-induced fluorescence of plants influenced by environmental stress with a microfluorescence imaging system and a fluorescence imaging lidar system. SPIE 3059:190-198
Sandermann H, Wellburn AR, Heath RL (1997) Forest decline and ozone. Springer
Schreiber U (1986) Detection of rapid induction kinetics with a new type of high-frequency modulated chlorophyll fluorometer. Photosynth Res 9:261-272
Schreiber U, Schliwa U, Bilger W (1986) Continuous recording of photochemical and non-photochemical chlorophyll fluorescence quenching with a new type of modulation fluorometer. Photosynth Res 10:51-62
Schulze ED, Lange OL, Oren R (eds) (1989) Forest decline and air pollution. Springer-Verlag
Siebke K, Weis E (1995a) Assimilation images of leaves of *Glechoma hederacea*: analysis of non–synchronous stomata related oscillations. Planta 196:155-165
Siebke K, Weis E (1995b) Imaging of chlorophyll *a* fluorescence in leaves: topography of photosynthetic oscillations in leaves of *Glechoma hederacea*. Photosynth Res 45:225-237
Takayama K, Goto E, Omasa K (2000) Diagnosis of photosynthetic injury caused by agricultural chemicals using chlorophyll fluorescence imaging. Proc XIV Memorial CIGR World Congress 2000:1436-1441

Wessman CA (1990) Evaluation of canopy biochemistry. In: Hobbs RJ, Mooney HA (Eds) Remote sensing of biosphere functioning. Springer, pp 135-156
Yunus M, Iqbal M (1996) Plant response to air pollution. Wiley